Published in "Nature doi:10.1038/nature10649, 2011"
which should be cited to refer to this work.

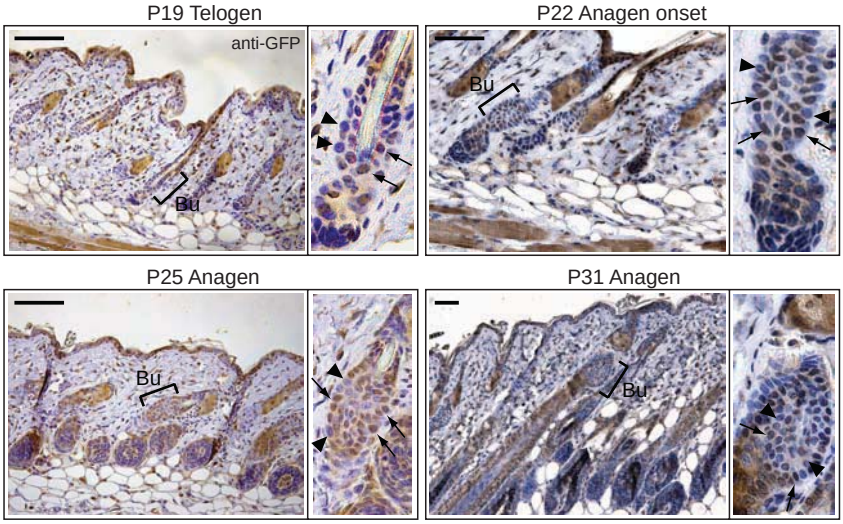

Supplementary Figure 1: Bulge stem cells are heterogenous in their clock.
Immunohistochemistry of venus-GFP in Per1-venus mouse backskin at different hair cycle stages shows venus^{bright} (arrow) and venus^{dim} (arrowhead) cells in the bulge (Bu, bulge). Scale bar, 100 μm.

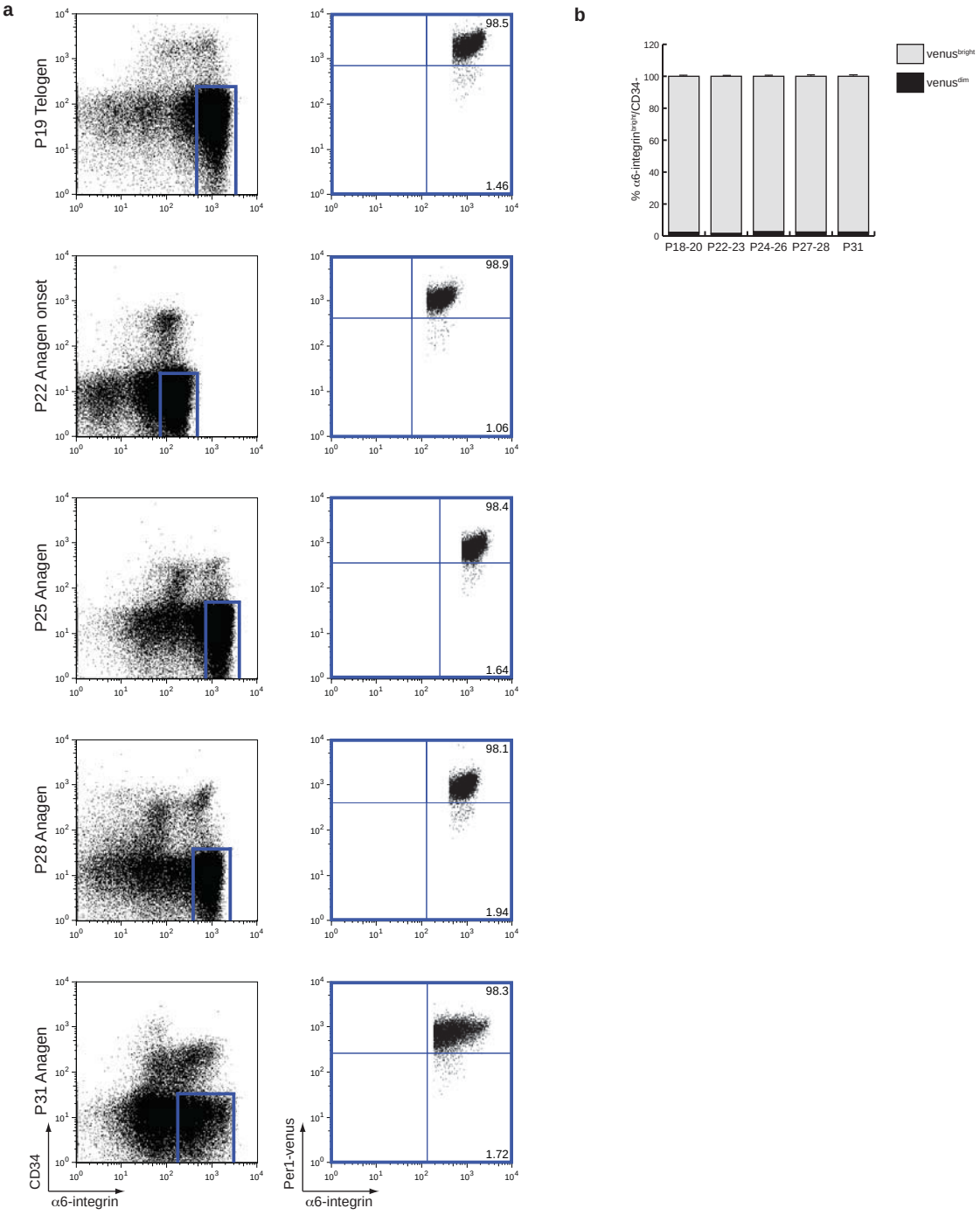

Supplementary Figure 2: Per1-venus expression is homogeneous in the basal epidermis during anagen. **a,b**, Quantification of venus^{bright} and venus^{dim} cells in the α6 integrin^{bright}/CD34- epidermal population of Per1-venus mice at different stages of the hair cycle (P19, P22, P25, P28 and P31) by FACS showed no changes in the percentage of venus^{bright} and venus^{dim} cells in the basal epidermis (mean ± s.e.m.; n ≥ 6).

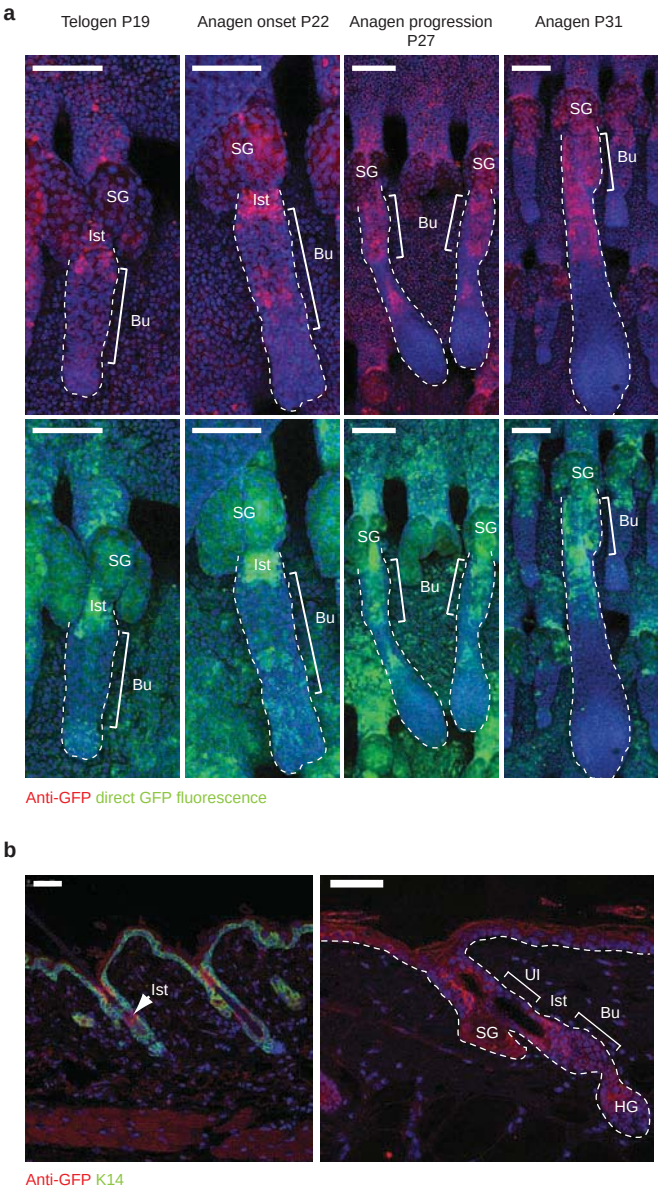

Supplementary Figure 3: Dynamic changes of Clock gene expression during the hair cycle in Per1-GFP reporter mice.

a, Whole mount immunostaining of mouse tailskin from Per1-GFP mice at different stages of the hair cycle (from P19 to P31) showed a steady increase of GFP^{bright} cells in the bulge compartment during anagen. Upper panel, anti-GFP staining; lower panel, direct GFP fluorescence. Scale bar, 100 μm. **b**, Immunostaining for GFP (red) and Keratin 14 (K14; green) revealed strong GFP expression in the isthmus region, which contains epSCs that feed into the epidermis and sebaceous glands. Scale bar, 50 μm. Bu, bulge; SG, sebaceous gland; Ist, isthmus; UI, upper isthmus; and HG, hair germ.

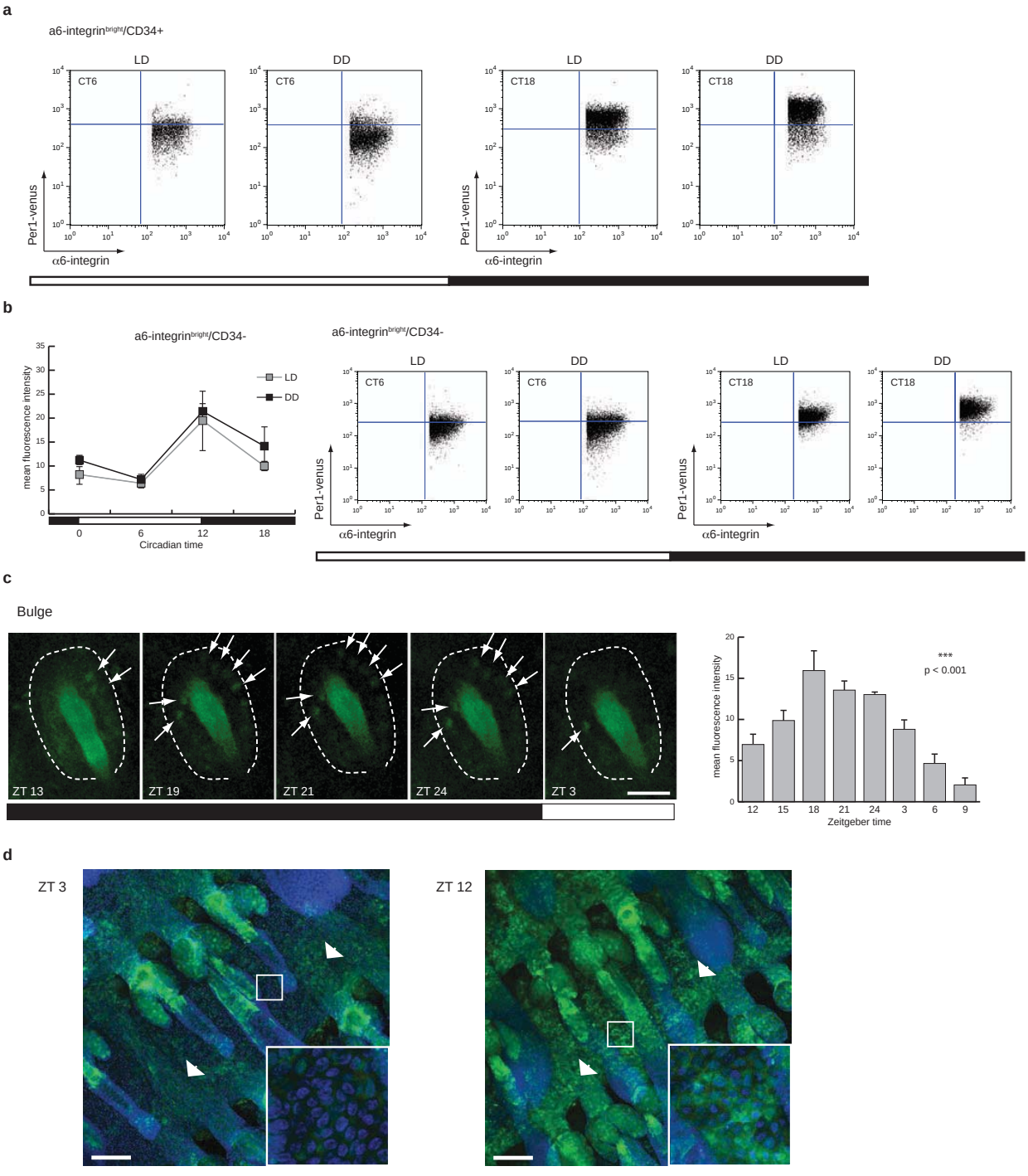

Supplementary Figure 4: GFP/venus expression changes in a circadian manner.
a, b, Comparison of venus mean fluorescence intensity in α6-integrin^{bright}/CD34+ bulge (**a**) and α6-integrin^{bright} /CD34- epidermal cells (**b**) from P27 Per1-venus mice kept under LD and DD conditions (one representative FACS profile is shown at CT6 and CT18 from each group; the gate to separate venus^{bright} from venus^{dim} cells was placed in all profiles according to the time point of brightest venus fluorescence intensity at CT12). The graph in **b** shows quantification of α6-integrin^{bright}/CD34- epidermal cells at 4 different time points by FACS (mean ± s.e.m.; n = 2). White and black bars represent subjective day and night. **c**, Timelapse confocal imaging of telogen backskin of Per1-venus mice reveals an increase in venus^{bright} nuclei in the bulge during the subjective night (from ZT13 to ZT24; arrows) Scale bar, 25 μm. Graph shows quantification of mean fluorescence intensity of venus^{bright} nuclei in the bulge over 24 hours (n = 5 nuclei; mean ± s.e.m.; *** $p < 0.001$ using Cosinor analysis) **d**, Whole mount immunostaining of mouse tailskin from Per1-GFP mice at Zeitgeber time ZT3 (3 hours of light) or ZT12 (12 hours of light) shows clear differences in GFP intensity in the basal epidermis (arrows and higher magnification)

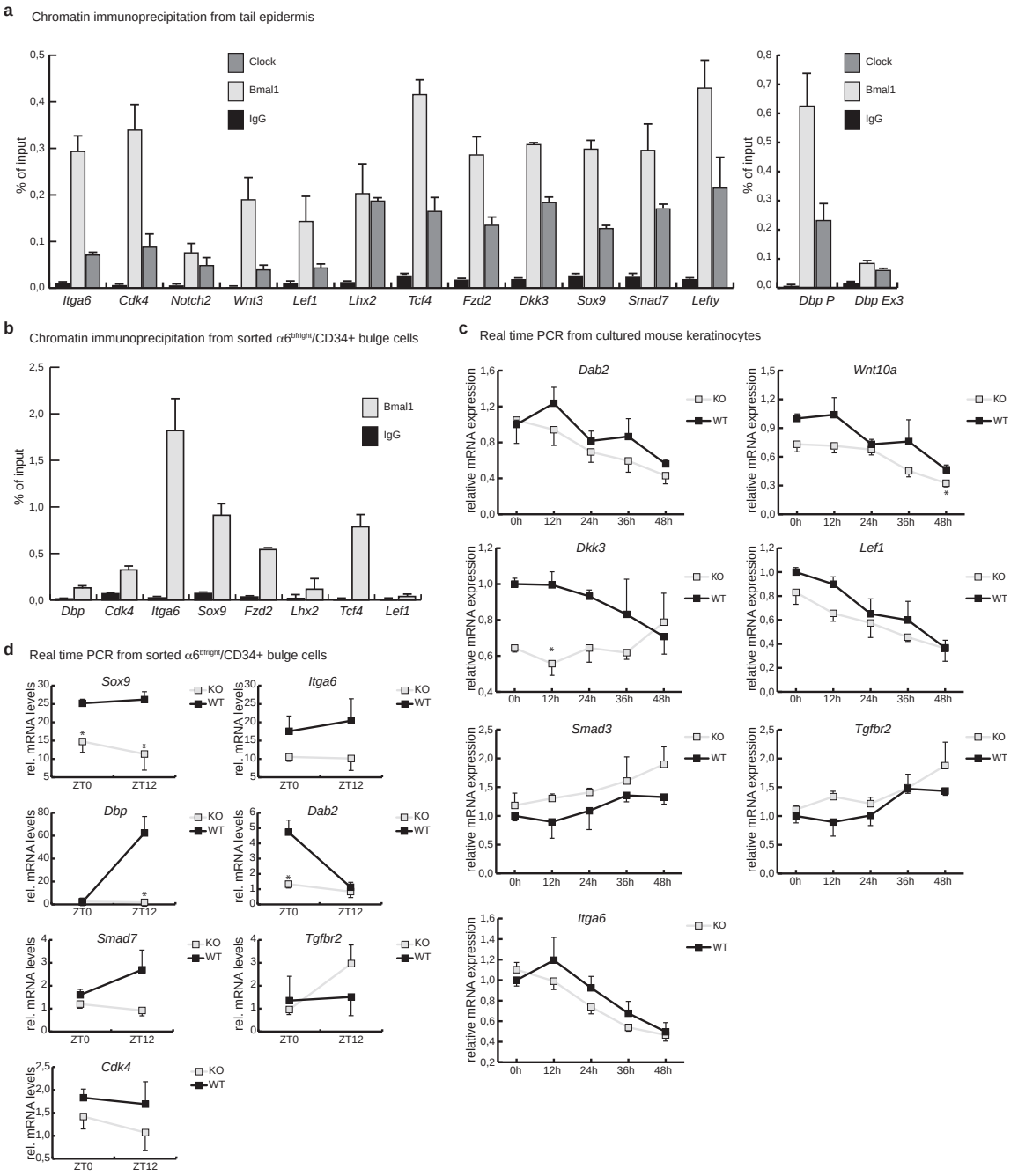

Supplementary Figure 5: Bmal1 modulates the response of epidermal cells to activation and dormancy cues.

a, ChIP from tail epidermis of Bmal1WT mice revealed binding of Bmal and Clock to E-box and E-box-like elements in the promoters of genes involved in adhesion, cell cycle, Notch, TGF-β and Wnt pathways. ChIP for Bmal1 and Clock in 2 regions of the circadian-regulated gene *Dbp* was used as positive (P, promoter) and negative control (Ex3, exon 3). (n = 3, mean ± s.e.m.). **b**, ChIP from FACS-purified bulge cells of Bmal1WT mice shows strong binding of Bmal to the promoters of genes highly expressed in the bulge SC compartment (n = 2; mean ± s.e.m.). Graphs in **a** and **b** show the percentage of immunoprecipitated DNA over the input. **c**, The differential expression of adhesion, Wnt and TGF-β pathway genes in primary keratinocytes isolated from newborn Bmal1WT (WT) and Bmal1KO mice (KO) was not statistically significant. Fold-change values are displayed as relative expression to Bmal1WT cells at 0h after normalization to *Pumilio1* (*Pum1*) (n = 3). Results are shown as mean ± s.e.m., * $p < 0.05$ (two-way ANOVA with Bonferroni post-test). **d**, Real time PCR of adhesion, cell cycle, Wnt and TGF-β pathway genes in FACS purified bulge cells of 9-month-old Bmal1WT (WT) and Bmal1KO mice (KO) at ZT0 and ZT12. Expression levels are shown as relative mRNA levels after normalization to *Pumilio1* (*Pum1*) (n =

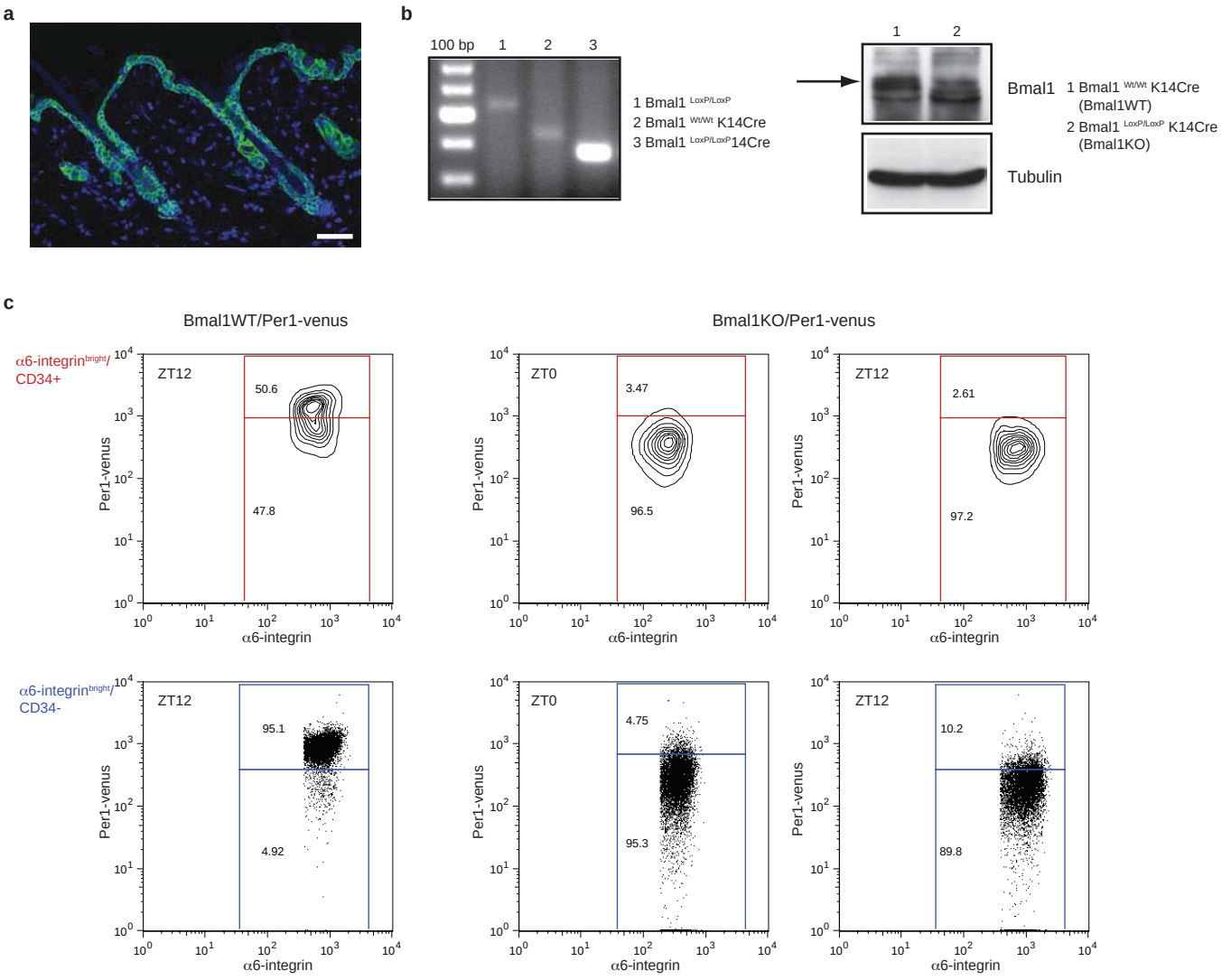

Supplementary Figure 6: Conditional deletion of *Bmal1* in the epidermis.
a, Immunostaining for Keratin 14 (green) to mark Cre-expressing cells in the epidermis. Scale bar, 50 μm. **b**, Efficiency of LoxP recombination in the epidermis of K14Cre/Bmal1$^{LoxP/LoxP}$ (Bmal1KO) mice was assessed by PCR from genomic DNA of epidermal cells (left panel; lane 1, conditional allele; lane 2, Wt allele; lane 3, recombined allele) and by western blot for Bmal1 in keratinocytes isolated from Bmal1WT or Bmal1KO mice (right panel; arrow). **c**, Conditional deletion of Bmal1 effects the expression of venus in the epidermis of Bmal1KO/Per1-venus mice. Quantification of venus^{bright} and venus^{dim} cells in the α6 integrin^{bright}/CD34+ bulge and α6 integrin^{bright}/CD34- epidermal population by FACS revealed a loss of venus expression in Bmal1KO/Per1-venus mice at ZT0 and ZT12 as compared to Bmal1WT/Per1-venus mice at ZT12 (numbers show percentages; n ≥ 3).

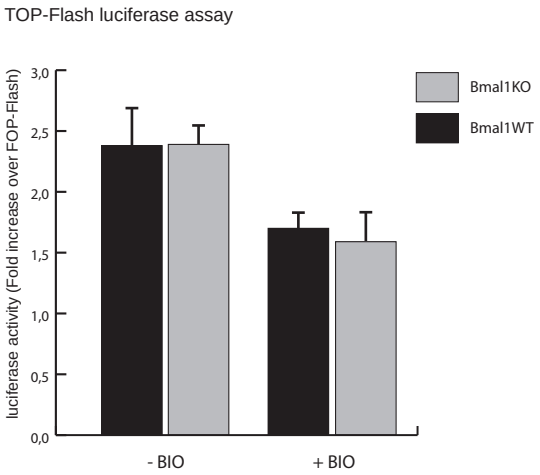

Supplementary Figure 7: Primary mouse keratinocytes did not respond to activation through canonical Wnt signaling.
Primary mouse keratinocytes of Bmal1WT and Bmal1KO mice transfected with TOP-Flash and FOP-Flash reporter plasmids were incubated for 24 hours in the absence or the presence of the canonical Wnt small molecular activator BIO (mean ± s.e.m.; n = 2).

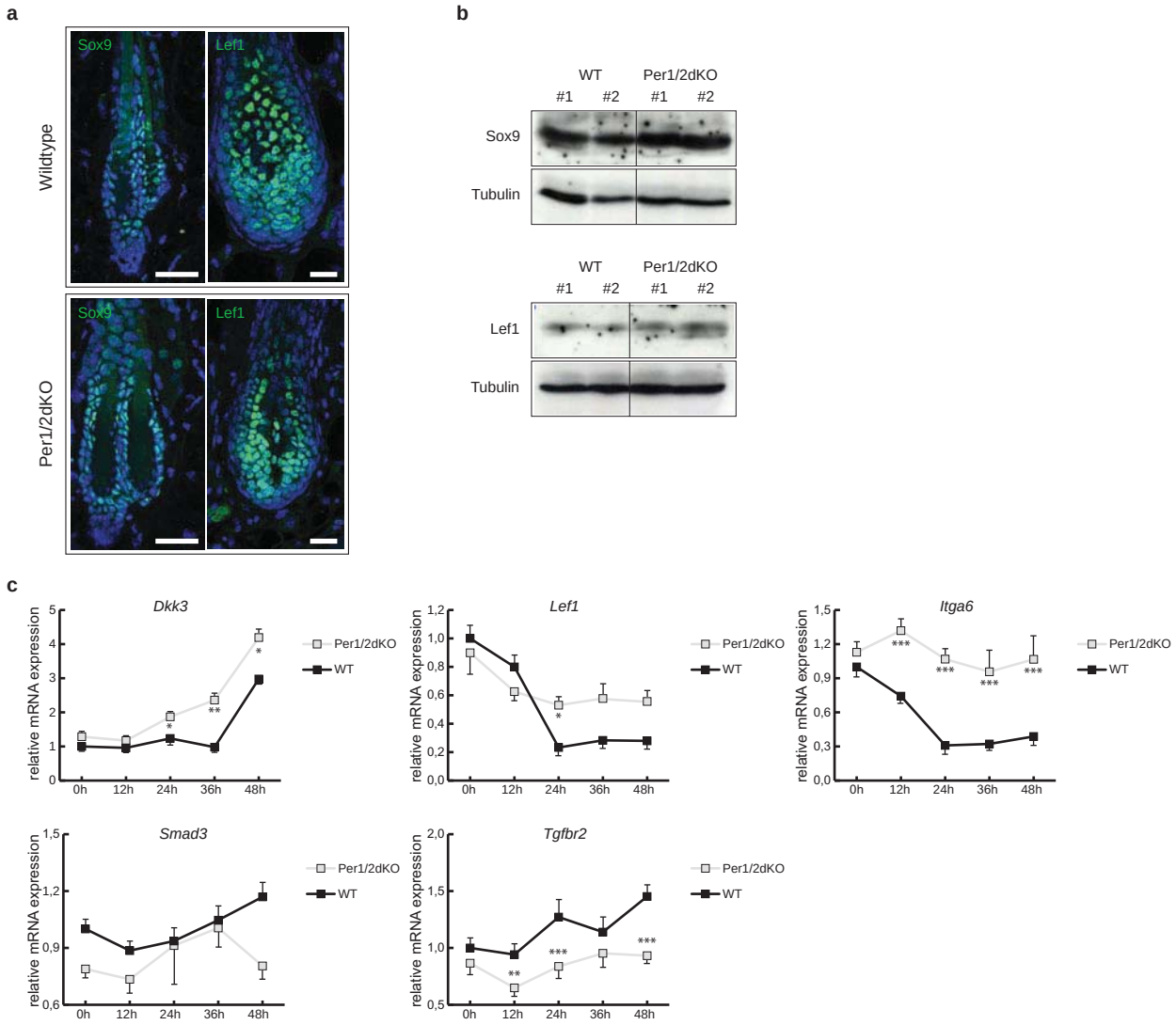

Supplementary Figure 8: Per1/2dKO epidermal cells show enhanced expression of Bmal1 targets.
a, Backskin of Per1/2dKO mice and wildtype control animals was stained for Lef1 and Sox9 (n ≥ 6). Scale bars, 25 µm. **b**, Protein extracts from tail epidermis of 6-week-old Per1/2dKO mice and wildtype control animals (WT) were analysed by western blot for the expression of Lef1 and Sox9. Lanes represent extracts from two WT and two KO animals (#1, #2). Tubulin expression was analysed as loading control. **c**, Real time PCR of adhesion, Wnt and TGF-β pathway genes in primary keratinocytes of Per1/2dKO and wildtype control animals (WT). Fold-change values are displayed as relative expression (mean ± s.e.m.) to WT cells at 0h after normalization to *Pumilio1* (*Pum1*) (n = 2). Results are shown as mean ± s.e.m., * $p < 0.05$, ** $p < 0.01$, *** $p < 0.001$ (two-way ANOVA with Bonferroni post-test).

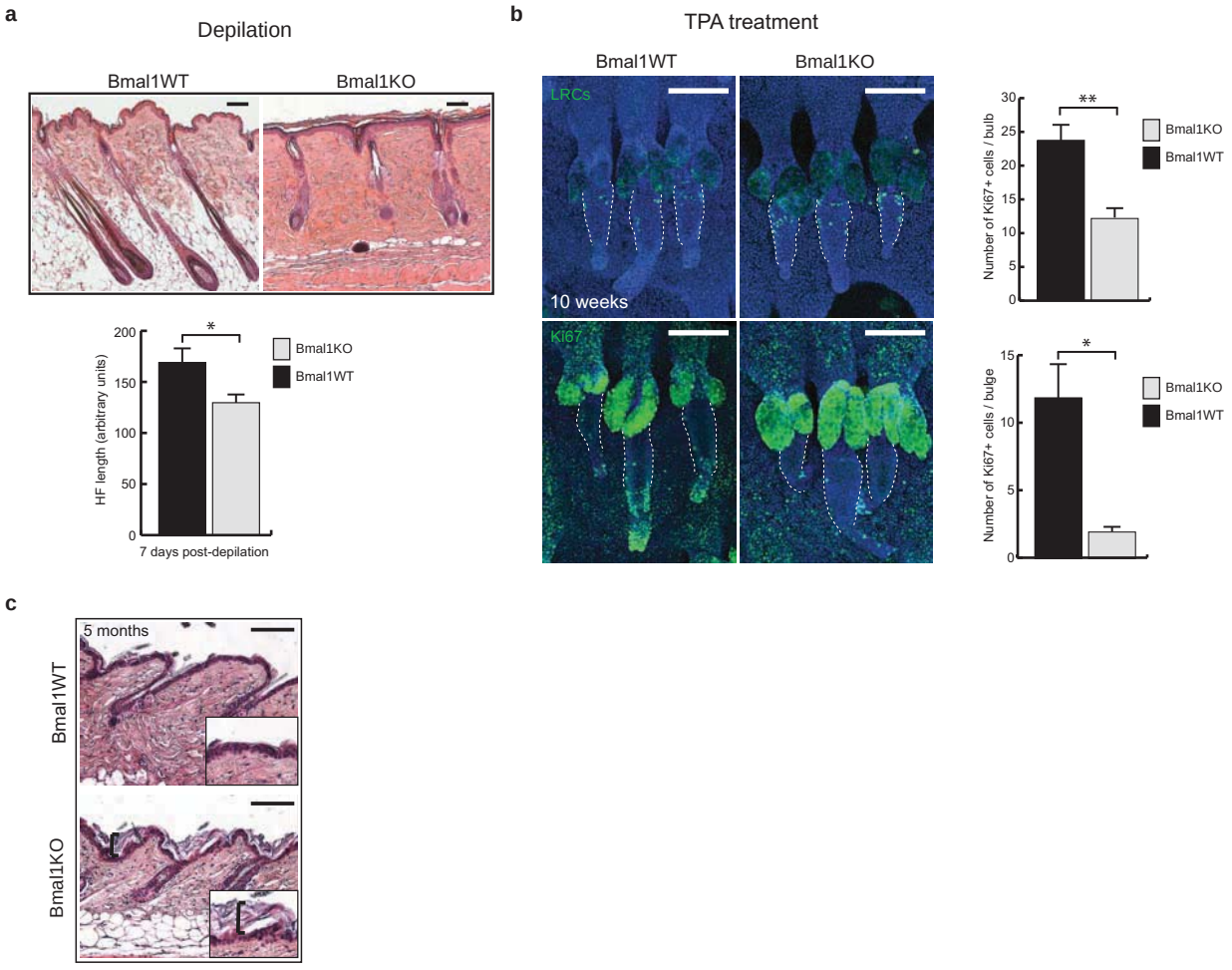

Supplementary Figure 9: Clock perturbation in vivo results in changes in the number of dormant bulge stem cells and premature tissue aging.
a, Depilation-induced anagen entry shows a growth delay in Bmal1KO mice (n ≥ 5). **b**, Wholemount immunostaining for BrdU (LRCs) and the proliferation marker Ki67 of 10-week-old Bmal1WT and Bmal1KO after 1 week of TPA treatment (n = 5). **c**, Histological analysis of 5 month old Bmal1WT and Bmal1KO mice. Scale bars 100 μm. Results are shown as mean ± s.e.m., * $p < 0.05$, ** $p < 0.01$ (two-tailed Student's t-test).

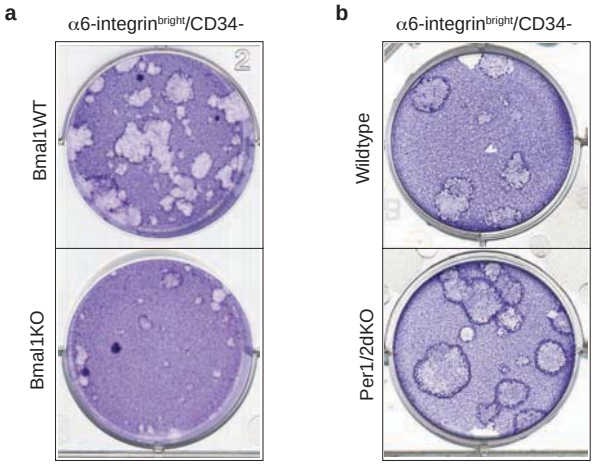

Supplementary Figure 10: Clock^{high} epidermal keratinocytes have an increased clonogenic potential.
a, b, Clonogenic assay of FACS-purified α6-integrin$^{bright/}$ CD34- epidermal keratinocytes from the backskin of (**a**) Bmal1WT and Bmal1KO mice or (**b**) Per1/2dKO mice and wildtype control animals (1x10^5 cells seeded on J2 3T3 feeder cells).

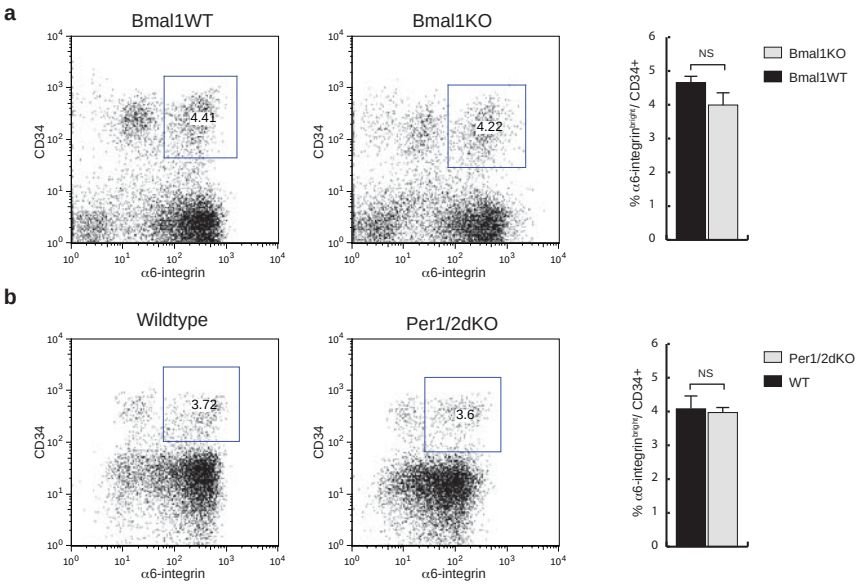

Supplementary Figure 11: Percentage of bulge stem cells is not altered in Bmal1KO and Per1/2dKO mice. **a, b,** FACS analysis of α6-integrin^{bright}/CD34+ bulge cells of (**a**) Bmal1WT and Bmal1KO mice or (**b**) Per1/2dKO mice and wildtype (WT) control animals show no differences in the percentage of bulge stem cells in 6-week-old animals (n = 4). Results are shown as mean ± s.e.m.; statistical significance was assessed by two-tailed Student's t-test. NS, not significant.

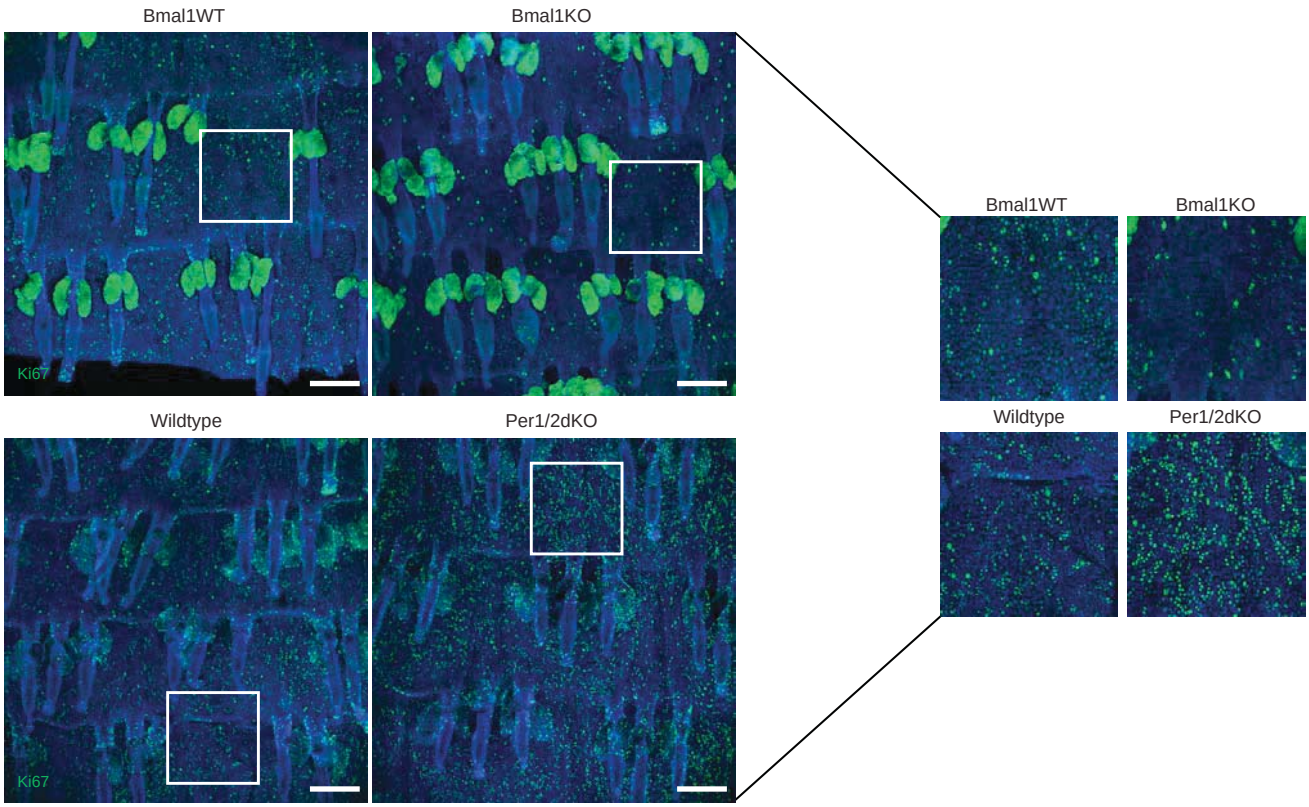

Supplementary Figure 12: Bmal1KO and Per1/2dKO mice show opposite phenotypes with regard to epidermal proliferation.
Whole mount immunostaining for the proliferation marker Ki67 shows lower expression of Ki67 in the epidermis of Bmal1KO mice compared to Bmal1WT mice, and enhanced expression in the epidermis of Per1/2dKO mice with regard to their wildtype controls. Scale bars, 100 µm. (Upper panel: unspecific staining in sebaceous glands was Ki67 antibody batch dependent).

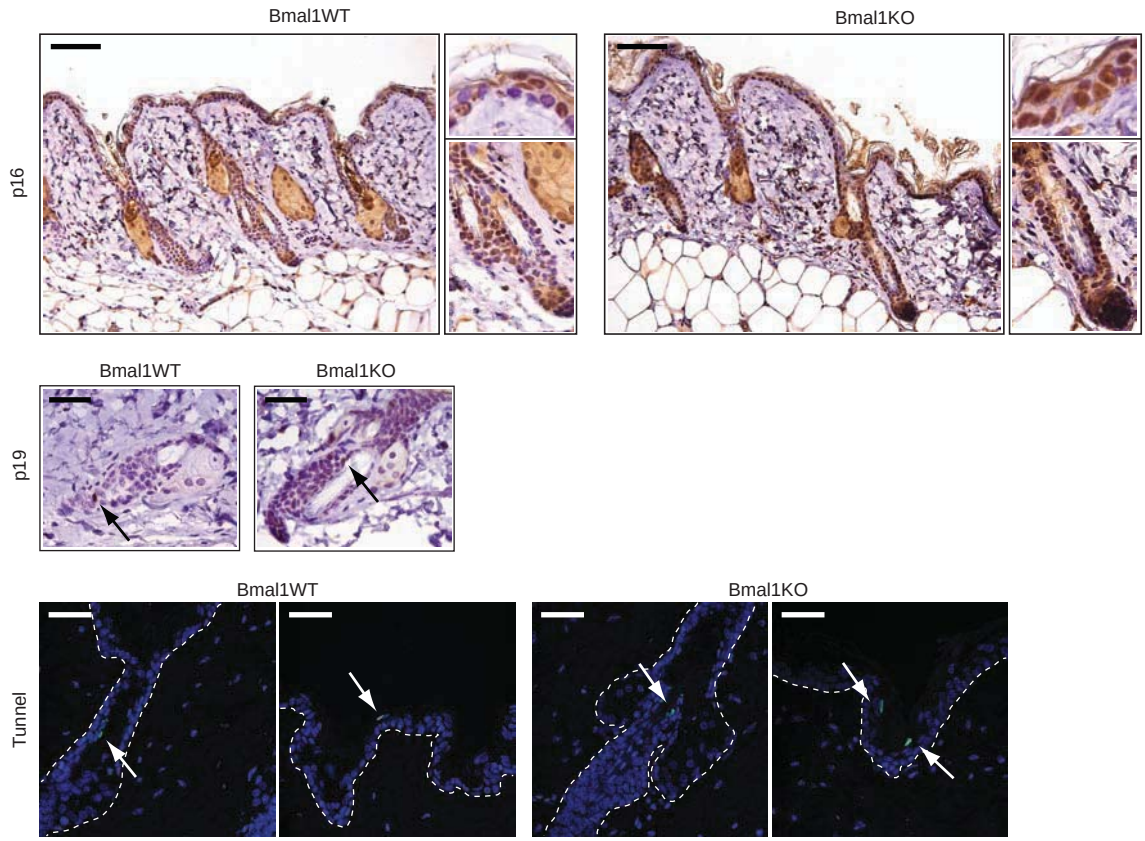

Supplementary Figure 13: Analysis of aged Bmal1KO mice for the expression of p16, p19 and apoptosis. Immunohistochemistry for p16 in 10-12-month-old Bmal1WT and Bmal1KO mice revealed enhanced expression of p16 in the epidermis and hair follicles of Bmal1KO mice. Cells positively stained for p19 (black arrows) were only occasionally observed in Bmal1WT and Bmal1KO mice in similar numbers. Similarly, apoptotic cells (Tunnel; green; white arrows) were only infrequently detected and located mainly to terminal differentiated areas of the hair follicle and the interfollicular epidermis. Scale bars, 50 μm.

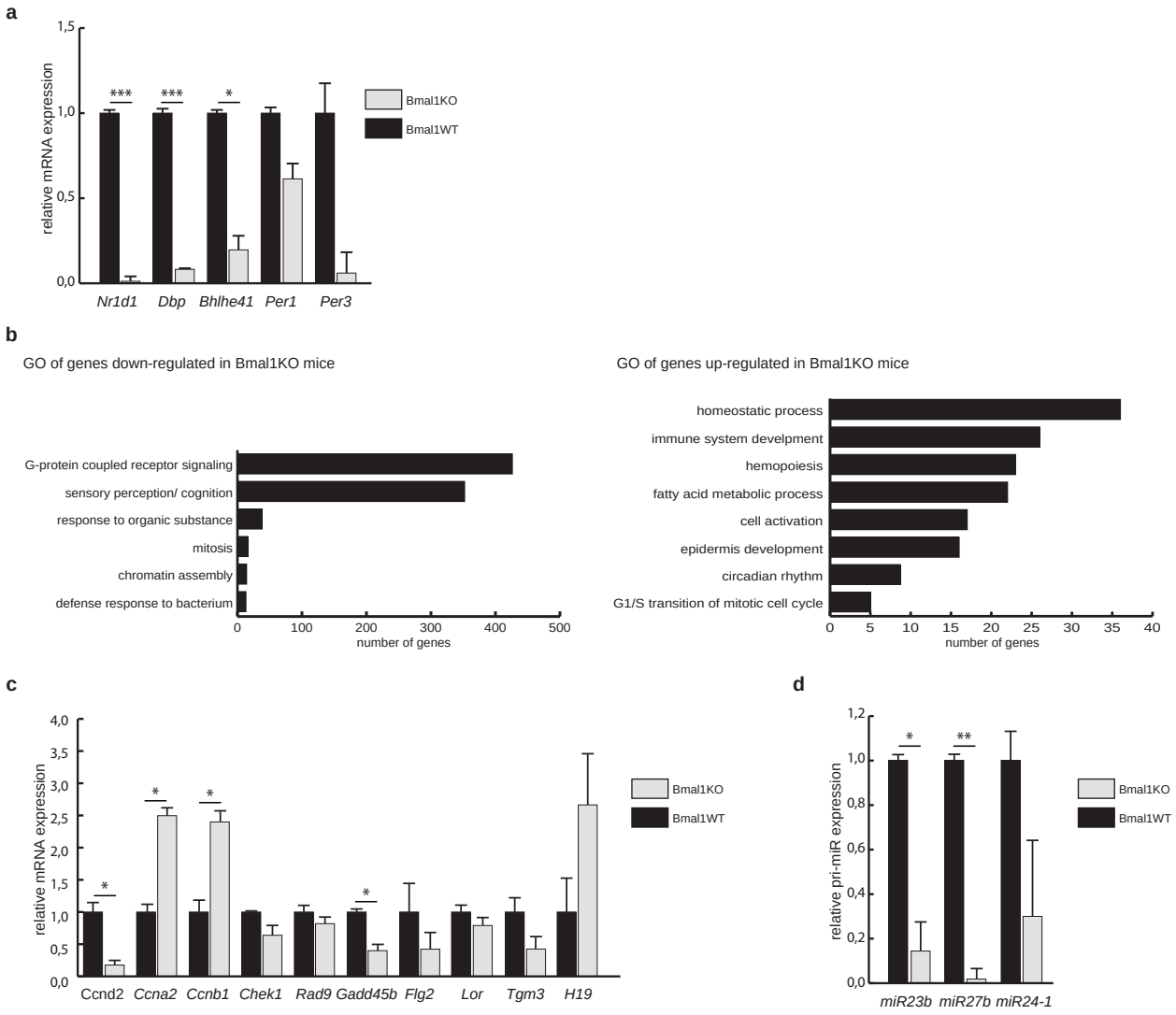

Supplementary Figure 14: Validation of microarray data comparing aged BMAL1WT and BMAL1KO mice. **a, c, d,** Validation of microarray data in FACS isolated α6 integrin^{bright}/CD34- epidermal cells from Bmal1KO and Bmal1WT mice by real time PCR (n = 2-3, for each group) shows differential expression of (**a**) several core circadian genes, (**c**) genes implicated in cell cycle, DNA damage and terminal differentiation and (**d**) the abundance of the pri-miRNAs *23b*, *27b* and *24-1*. Fold-change values are displayed as relative expression to Bmal1WT cells after normalization to *Pumilio1* (*Pum1*), or *18S*-rRNA. Results are shown as mean ± s.e.m., * $p < 0.05$, ** $p < 0.01$, *** $p < 0.001$ (two-tailed Student's t-test). **b**, Graphic depicts GO enriched biological processes of genes up- and down-regulated in Bmal1KO mice. (Fold change ≥1.4 or ≤-1.4; p-value ≤ 0.05).

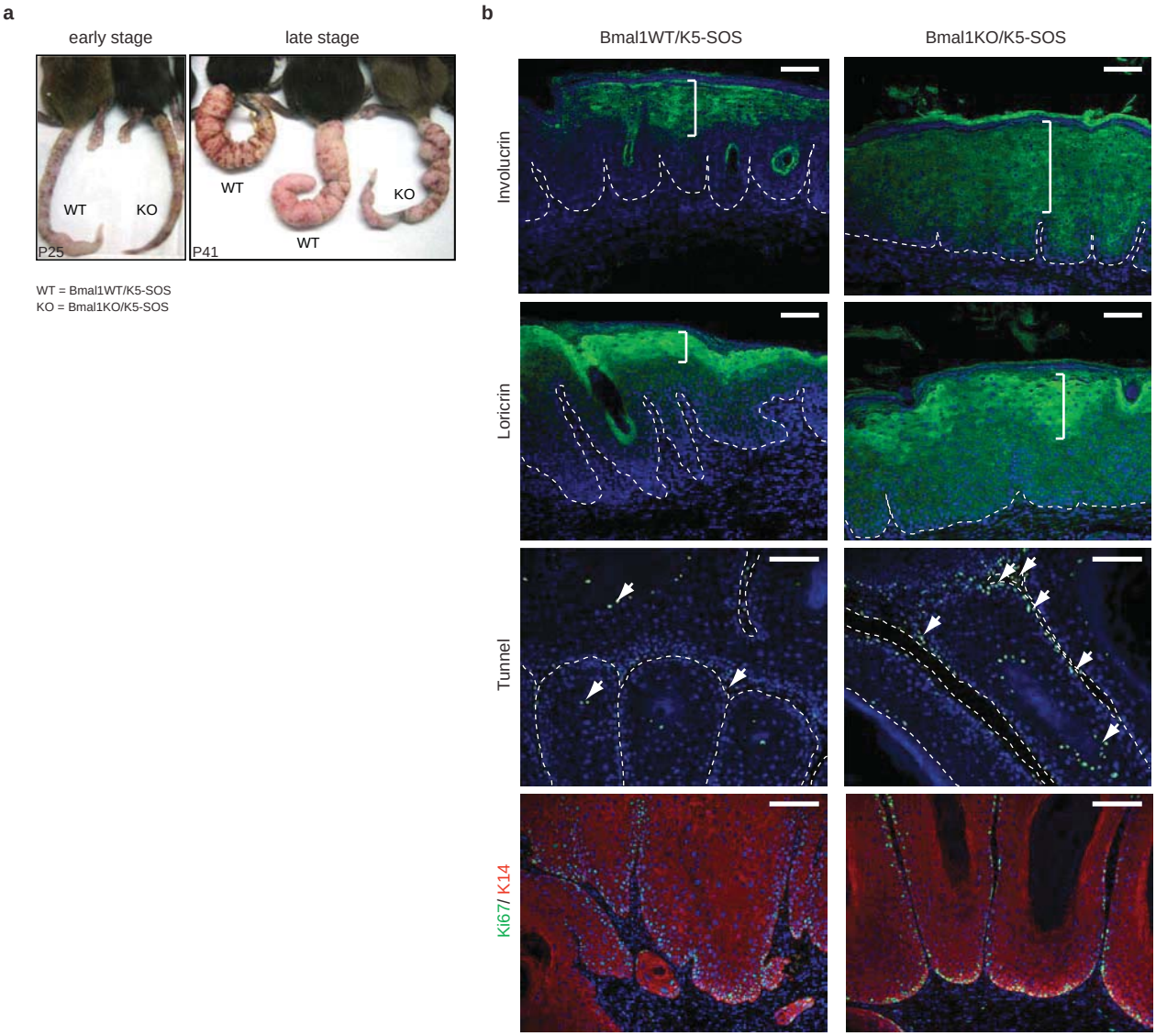

Supplementary Figure 15: Loss of *Bmal1* reduces the development of squamous tumors.
a, Bmal1KO/K5-SOS mice developed fewer neoplastic lesions compared to Bmal1WT/K5-SOS littermates at early and late stages. **b**, Immunostaining of tumors of Bmal1WT/K5SOS and Bmal1KO/K5-SOS mice for terminal differentiation (Involucrin, Loricrin), apoptosis (Tunnel; arrows) and proliferation (Ki67). Scale bars, 100 μm.

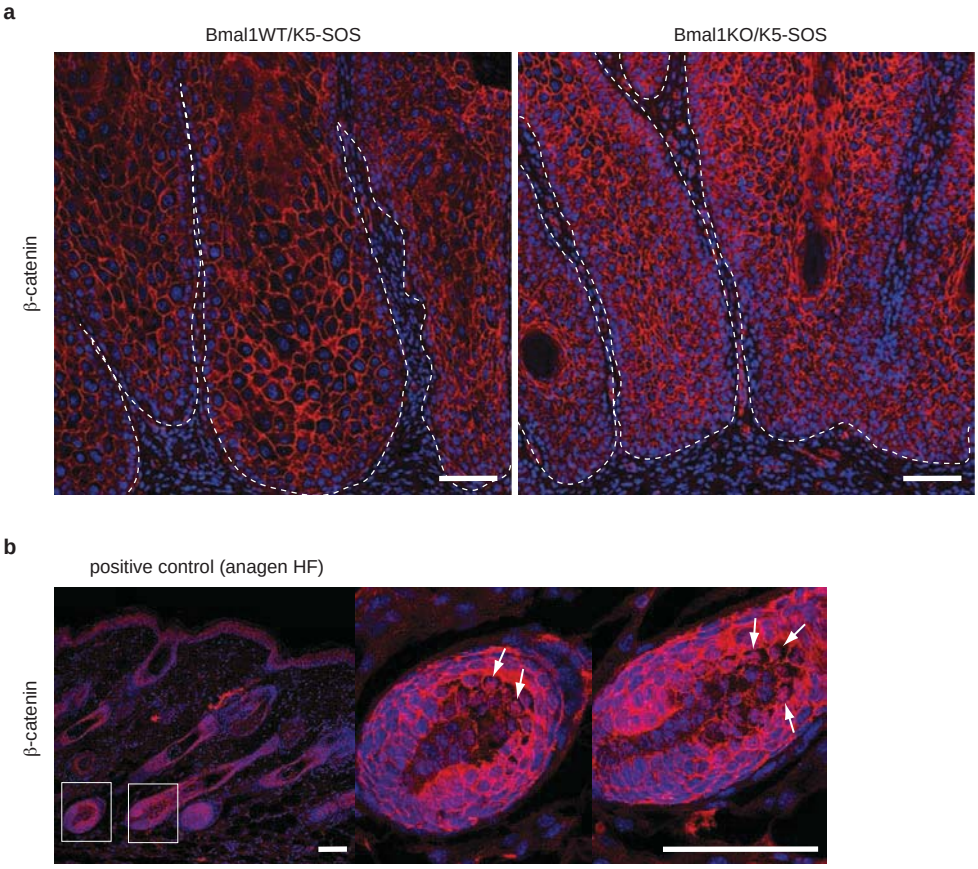

Supplementary Figure 16: Absence of nuclear β-catenin in K5-SOS induced tumors.
a, Immunostaining of sections from squamous tumors for β-catenin (red) shows no nuclear localization of β-catenin in K5-SOS induced tumors. **b**, Anagen hair follicle stained for nuclear β-catenin (arrow) was used as positive control to verify the staining protocol. DAPI (blue), scale bar, 75 μm.

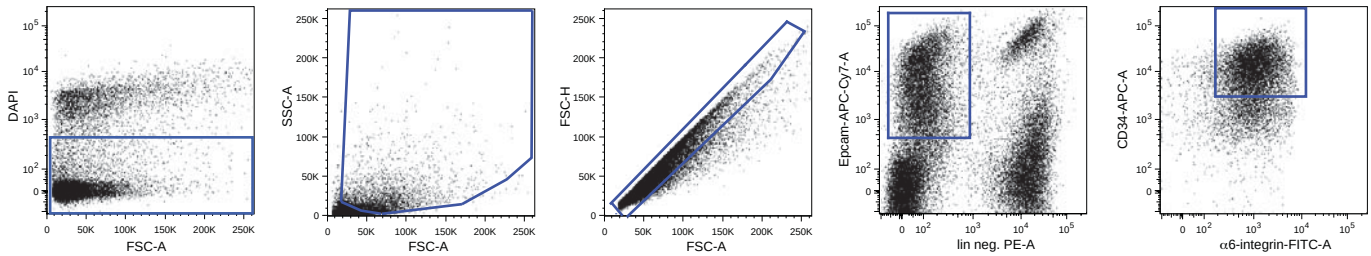

Supplementary Figure 17: Gating strategy for FACS analysis of K5-SOS induced tumors. Viable cells were selected by DAPI exclusion (gate 1), contaminating fibroblasts were excluded by forward and side scatter (gate 2), doublets were discarded in gate 3, epithelial cells were selected in gate 4 by a combination of a lineage negative markers in PE (CD31, CD45 and CD140a) and a positive marker (Epcam APC-Cy7), and $\alpha6^{bright}$/CD34+ tumor-initiating cells were selected in gate 5.

Supplementary Table 2

Gene	Chromosome	Distance from transcriptional start site	Location	Motif	Validated by ChIP
TGF-β pathway					
Tgfb1	7	- 642	Promoter	CACGTG	no
Tgfb2	1	- 50/ + 440	Promoter/Exon1	CACGTG /AACGTG	no/ no
Smad7	18	- 4839/ -177	Promoter/ Promoter	CACGTG/ CACGTG	yes/ no
Smad9	3	- 2797/ + 262	Promoter/ Intron 1	CACCTG/ CACGCG	no/ no
Smurf2	11	- 4687/ - 3945	Promoter/ Promoter	CACGTG/ CACCTG	yes/ no
Lefty	1	- 297	Promoter	CACGTG	yes
Wnt pathway					
Dkk1	19	- 413	Promoter	AACGTG	no
Dkk3	7	- 874	Promoter	CACGTG	yes
Wnt3	11	- 2940/ - 400	Promoter/ Promoter	CACGTG/ CACGTG	no/ yes
Wnt10a	1	- 2533/ - 1410	Promoter/ Promoter	CACGTG/ CACGTG	no/ no
Lef1	3	- 4917/ - 4468/ - 4098 - 3243/ - 2501/ - 490	Promoter/ Promoter/ Promoter Promoter/ Promoter/ Promoter	CACGTG/ CACGTG/ CACGTG CACGTG/ CACGTG/ CACGTG	yes/ no/ no no/ no/ no
Ctnnb1	9	- 2596	Promoter	AACGTG	no
Dab2	15	- 2842/ - 1247	Promoter/ Promoter	AACGTG/ AACGTG	no/ no
Fzd2	11	- 361	Promoter	AACGTG	yes
Tcf4	18	- 2914	Promoter	CACGTG	yes
Sox9	11	- 44	Promoter	AACGTG	yes
Lhx2	2	- 4668/ -2591/ - 2040	Promoter/ Promoter/ Promoter	CCCGTG/ CACGTG/ AACGTG	yes/ no/ no
Notch pathway					
Notch2	3	- 2687	Promoter	CACGTG	yes
Hes1	16	- 1809/ - 1014	Promoter/ Promoter	CACGTG/ CACGTG	no/ no
Adhesion/ Cell cycle/ others					
Itga6	2	- 4760/ - 3064 - 1689/ + 150	Promoter/ Promoter Promoter/ Exon1	AACGTG/ AACGTG CACGTG/ AACGTG	no/ no no/ yes
Cdk4	10	- 251/ - 197/ -177 - 90/ + 414	Promoter/ Promoter/ Promoter Promoter/ Intron 1	CACGTG/ CACGTG/ CACGTG CACGTG/ AACGTG	yes/ yes/ yes no/ yes
Wee1	7	- 656/ - 442 - 11/ + 186	Promoter/ Promoter Promoter/ Exon1	CACGTG/ AACGTG CACGTG/ CACGTG	yes/ no no/ no
Bmpr1a	14	- 4916	Promoter	AACGTG	no
Foxo3a	10	- 2435	Promoter	CACGTG	no

Gene promoters analyzed, but no binding sites for Bmal/ Clock found:

Delta1, Filaggrin, Fzd3, Gli2, Hey1, Involucrin, Jagged1, Lgr5, Ltbp2, Ltbp3, Ltbp4, Nfatc1, Notch1, Sfrp1, Smurf1, Tcf3

Supplementary Table 4

Real time PCR primer

Gene	Forward	Reverse
Bhlhe41	CTGCCCGAACATCTGAAATTGA	GCTGCTCAGTTAAGGCTGTTAG
Ccna2	CTTTACCCGCAGCAAGAAAAC	ACGTTCACTGGCTTGTCTTCTA
Ccnb1	CTCAGGGTCACTAGGAACACG	AGCTCTTCGCTGACTTTATTACC
Ccnd2	CTGTGCGCTACCGACTTCAA	CACATCAGTGTGGGTGATCTTG
Cd34	AAGGCTGGGTGAAGACCCTTA	TGAATGGCCGTTTCTGGAAGT
Cdkn2b (p15)	CCCTGCCACCCTTACCAGA	CAGATACCTCGCAATGTCACG
Chek1	GTTAAGCCACGAGAATGTAGTGA	GATACTGGATATGGCCTTCCCT
Dab2	AGGCCAAGCTAATCGGTATTGA	AATGTTGACCCAGATTCTTTGCT
Dbp	CCTGATCCCGCTGATCTCG	CAGGCACCTGGACTTTCCTT
Dkk3	CTCGGGGGTATTTTGCTGTGT	TCCTCCTGAGGGTAGTTGAGA
Flg2	GCCAACTGTCCAGTCTTGTTT	GCCTTTCATTAGGGCTGAATCC
Fzd2	GTTCTTCTCGCAAGAGGAGAC	TCGCTGCATGTCCACTAAATAG
Gadd45b	CAACGCGGTTCAGAAGATGC	GGTCCACATTCATCAGTTTGGC
H19	AGGATGACAGGTGTGGTCAA	TGAGTGAGTGGGTGGACAAT
Itga6	TGCAGAGGGCGAACAGAAC	GCACACGTCACCACTTTGC
Lef1	TGTTTATCCCATCACGGGTGG	CATGGAAGTGTCGCCTGACAG
Lor	GATCGTCCCAACAGTATCAGTG	TGCTGAGAGGAGTAATAGCCC
Ltbp2	CTGATGTCCAACGCTTTGCC	GTGGGGGTGAAGACGACTTT
Mki67	ATCATTGACCGCTCCTTTAGGT	GCTCGCCTTGATGGTTCCT
Nr1d1	TACATTGGCTCTAGTGGCTCC	CAGTAGGTGATGGTGGGAAGTA
Per1	ACCAGGTCATTAAGTGTGTGC	CTCTCCCGGTCTTGCTTCA
Per3	AAAAGCACCACGGATACTGGC	GGGAGGCTGTAGCTTGTCA
Pum1	AGGCGTTAGCATGGTGGAGTA	TCCATCAAACGTACCCTTGTTC
Rad9	CACTGCAAGTATGGGGTCAAG	GCAATAAGTGAGGGCATGAGG
Smad3	CCCCCACTGGATGACTACAG	TCCATCTTCACTCAGGTAGCC
Smad7	GAAACCGGGGGAACGAATTAT	CGCGAGTCTTCTCCTCCCA
Sox9	GAGCCGGATCTGAAGAGGGA	GCTTGACGTGTGGCTTGTTC
Tcf3	ACGAGCTGATCCCCTTCCA	CAGGGACGACTTGACCTCAT
Tgfbr2	AGTGATGTCATGGCCAGCGAC	CGCAGACTTCATGCGGCTTCTC
Tgm3	TCAGTGCTCCCATCGGATTG	GGCGTGGTTACTCATAAAGACAT
Wnt10a	GCTCAACGCCAACACAGTG	CGAAAACCTCGGCTGAAGATG
Wnt3a	CTCCTCTCGGATACCTCTTAGTG	GCATGATCTCCACGTAGTTCCTG
miR primer (Sun et al., 2009)[48]		
Pri-miR-23b	TTCTAAAGGAGGCTGCACTGC	AAATCAGCATGCCAGGAACCCAAGC
Pri-miR-27b	GTTCTAAAGAGGGATTACCAC	TGGTGAGCATCTTTGAAGGCTGTTG
Pri-miR-24-1	CTAAAGGGTCCAGGTCTCCATG	CTGAGCCAGTGTGTGAAATGAGAAC
18S-RNA	CCTGGATACCGCAGCTAGGA	TCTAGCGGCGCAATACGAATG

Supplementary Table 5

Chromatin immunoprecipitation primer

Gene	Primer name	Forward	Reverse
Dbp	Dbp_P	ACACCCGCATCCGGTAGC	CCACTTCGGGCCAATGAG
Dbp	Dbp_E3	CGTGGAGGTGCTTAATGACCTTT	CATGGCCTGGAATGCTTGA
Dbp primer (Ripperger et al., 2006)[49]			
Wnt3	Wnt3_UP	CAACCCCTTTGCTTTCTAG	GACACCCCCTTCCCAGTC
Lef1	Lef1_farUP1	CAGTGTACTGTAACAGTG	CTTCTTCCAGCCTGCTTC
Dab2	Dab2_farUP	CACTATGGAAAACGGGAC	CTCTTTGTTATTACACTTC
Dab2	Dab2_UP	GAACCAGGACTGCACACT	GGAGGACACAAAAGCATC
Notch2	Notch2_farUP	CACTCCAACAATTCAACAG	ACCCAACTTTAACTTCTG
Itga6	Itga6_E1	GCTTCTAGCCCGGCTGGG	GAACTCACAGCCGCTTGTC
Cdk4	Cdk4_UP1	CTTGTGCTCCACCCTCTC	CTGACGGCCACGTGACCTG
Cdk4	Cdk4_I1	GTGATCCTCTTTGTGCCTAG	GCCAACGCGATCAGCAAC
Lhx2	Lhx2-farUP1	CAGATCGCTGCAGGGAGAAG	GGTCATACCATACAGAGAT
Tcf4	Tcf4_farUP	CCAAGAAGTCTGCGGTGA	CCAGCGATCATTAGTTACC
Fzd2	Fzd2_farUP	GCTCTTGTACCTCAGAGG	GCTCAGTCCGTGATTGCT
Smad7	Smad7_farUP	GGACATCAGCTCTGAATC	AGGCTGGTATGATGATGG
Lefty	Lefty_UP	GCAGAGAACGTGAGACCTC	TGTTAGCCATATACTTCACC
Dkk3	Dkk3_UP	TGCTGCAACGGACAGACC	CTCTCCGCATCTCCTGATC
Sox9	Sox9_UP	ATCCGGTCCAATCAGCGAC	CTCTCCGACTTCCAGCTCAG